AERODYNAMIC STUDY OF NEW ENGINE / AIRFRAME INTEGRATION CONCEPTS

Ph. MOGILKA
Ph. COLIN
N. ESTEVE
Aerodynamics Design Department
AEROSPATIALE - Avions
316, route de Bayonne 31060 TOULOUSE CEDEX 03
FRANCE

ICAS-94-6.4.2

Abstract

In the context of minimizing engine / wing integration aerodynamic effects, studies of VHBR turbofans and thrust vectoring concept are new challenges faced by Aerospatiale Avions. Two dependant tools are used for this purpose : TPS wind tunnel tests and EULER CFD.

This paper deals with their use for two different exercises : VHBR integration on a twin and thrust vectoring effect on a four engines aircraft.

Main results due to intense use of both tools indicate :
- limited penalties for the integration of a VHBR engine on a twin, but care shall be given to the pylon leading edge shape. Engine axial positioning, within reasonable limits, seems second order effect.
- potential drag benefits at cruise with down pointing thrust vector on a given four engines aircraft. A performance loop precises that the optimum is reached with -4° deviation. No clear explanations could be found in wing pressure analysis. CFD brings complementary informations helping for a better understanding of the result.

CFD importance and use have grown up during the past years (preselection of the configuration, simulation quality checking, complementary results understanding). But, experimentation will always remain essential for complex, viscous and unsteady flows. The two technics have reasonably learned to work together.

1. Introduction

In the AIRBUS group, Aerospatiale Avions is responsible for the engine airframe integration. On an aerodynamic point of view, this task includes the search for minimizing aerodynamic effects (lift loss and drag increase) due to engine jet effect that should be faced. Two different and now more and more dependant tools are used to complete this work : one is the wind tunnel technic including jet simulation by TPS (Turbofan Propulsion Simulator), the other one is the CFD approach through the use of the SESAME Euler solver developed by ONERA. Both methods are used on the same configurations of engine / nozzle / pylon / wing integration. Depending on the specific subject of study, CFD prepares the wind tunnel test by selecting some configurations among a large panel of choice, or CFD could help for the better understanding of wind tunnel results.

The hereafter paper deals with this dual methodology for a typical study by :

- quickly reviewing the powered engine wind tunnel technic
- giving a short overview of the CFD tool
- detailing a VHBR engine integration example
- expressing the thrust vector deviation impact on aerodynamic as determined through a three years experimental and CFD study.

2. Experimental technic

2.1 Hardware

The experimental technic used in Aerospatiale for the determination of the jet effect level at cruise is based on the TPS simulation. This know-how has been developed in cooperation between Aerospatiale and ONERA for more than fifteen years now.

In this methodology, the jet effect is defined as being the aerodynamic coefficient difference between an engine / airframe integration configuration run with through flow nacelle (TFN) one time and with TPS another time, and excluding pure thrust effects.

In this context, an half model is particularly well adapted.

The TPS is fitted with cowlings representing the lines of the studied nacelle. In the case of long fan duct nacelle with internal mixed flow, two options could be used (fig 1). One possibility is to draw a long core cowl which exit is out of the fan cowl : this technic separates the core and fan working and has been used by Aerospatiale till two years ago. The other possibility is to design a short core cowl having the same exit station than the full scale one and creating internal free mixing. With the help of CFMI, this has been used for the last two years for the A340 and it can be considered as the new standard of design for long duct mixed flow TPS nacelle.

Separate flow nozzle | Mixed flow nozzle

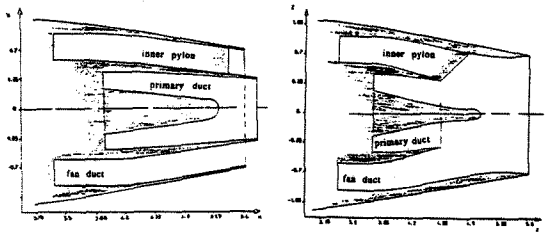

- figure 1 -

The TPS is driven by compressed air which is fed through the wing and the engine pylon. These parts of the model are equipped with numerous static pressure taps.

Model scale is a compromise between wind tunnel test section size and available TPS diameter versus real engine one. The dual AIRBUS family of aircraft including twin and four engines are represented by an 1/17.5 half model which can handle 104 mm, 142 mm or 180 mm TPS depending on the tested configuration.

2.2 Test procedure

The target of such tests is to determine the aerodynamic effect of the engine integration and, in this paper, the effect of the jet coming out of the engine exit at cruise. For this reason, any kind of engine thrust, which has not to be considered as aerodynamic effect, shall be removed from balance measurements in wind tunnel.

The estimate of these parasitic forces components are realized during a dedicated calibration test in an altitude bench before the effective wind tunnel test.

Before any TPS test, the bench deviation is checked by ASME nozzles. Many parameters are measured : fan and core mass flows, nacelle thrust on engine and vertical axis, total pressure and temperature behind the fan and the core oriented grid vanes, static pressure in the fan duct at the mixing or/and the exit stations. These measurements are realized for different TPS rotating speeds and upstream total pressure versus exit static pressure ratios.

All these informations computed together lead to the determination of one couple of law for each upstream total to exit static pressure ratio. They are valid for one given simulator within one set of cowlings. Any disassembly of the cowlings could introduce model leakages and so compromises the validity of the calibration laws. If during the installed test, a temperature or pressure probe becomes out of order, then the calibration laws shall be recomputed without this instrumentation.

Once the calibration test is completed, the nacelles are installed on the wing model for the wind tunnel test.

For the specific subject of the paper, Aerospatiale use the ONERA S1 transonic wind tunnel. The half powered model is set on the ground of the test section which is included in a 8 meters diameter circle.

Forces and moments are measured with a six components balance. Wing static pressures and TPS rakes total pressures are scanned with PSI devices.

Powered nacelles thrust and ram drag during wind on test are calculated with calibration data. Forces are subtracted from global balance measurements taking into account test Mach number, TPS fan nozzle pressure ratio, model geometry for engines setting angles and the usual aerodynamic wind tunnel corrections.

Each specific configuration shall be associated to a well known reference. It is tested time to time during the campaign and at least once per week. Differences of aerodynamic coefficients between the specific configuration and the reference could be directly applied to the aircraft polars as the foreseen jet effect.

This test procedure has been developed and applied by Aerospatiale for now more than fifteen years. This has been successfully used for all AIRBUS family aircraft development programs including several engine types.

Two examples of the use of this methodology are given in paragraphs 4 and 5. They illustrate the interest of this know how in the development of such studies.

3. CFD approach

Aerospatiale use the SESAME code developed by ONERA to perform CFD analysis for this kind of study. It is based on an EULER solver which requires a volumic grid generation.

3.1 Grid generation

This operation is based on the ICEM-CFD software developed by Control Data in cooperation with Aerospatiale [3] [4]. This tool is operated in interactive mode on a workstation and allows highly flexible mesh generation around numerous different configurations.

The mesh is produced during two complementary steps. First one defines the grid topology, i.e. the splitting of the calculation domain into interconnected elementary blocks surrounding the object to be meshed. The second step deals with the discretization. The operator can select the number of nodes on principal edges : suitable distribution allows to tighten the cells close to the body and obtain a regular grid within the volume. Other edge distribution is automatically computed. Subfaces and interior of the domains are then meshed by transfinite interpolation. Correct choices during topology and discretization steps directly condition the quality of the final grid.

In the aim of reducing the CFD loop delay, Aerospatiale has developed the COMAK tool allowing to use ICEM-CFD in automatic mode. All the mesh generation operations are recorded on a command file in which the CAD surface file names could be modified. The new mesh based on this new geometry is obtained by rerunning the command.

The resulting files are composed by the point coordinates of the mesh and by a complete description of the topology. This last item is largely used by the CFD code and its interfaces.

3.2 EULER solver

The EULER solver used by Aerospatiale for the subjects dealt in this paper is the SESAME code developed by ONERA. It solves the time dependant 3D EULER equations using a finite volume formulation.

This code has been initially developed in a cell vertex version [5] and recently modified to the cell centered option. This last development is the today used one [6]. Numerical fluxes are computed through a centered scheme. Time integration is realized by a Runge-Kutta four step scheme. Turkel-Jameson artificial viscosity is added for centered scheme stability purpose. Convergence is accelerated by the use of a local time step and an implicit residual smoothing phase.

Boundary conditions treatment is realized by introducing fictitious cells at the border of each block and is based on characteristic relations.

In the particular context of this paper, engine simulation requires specific boundary conditions (fig 2).

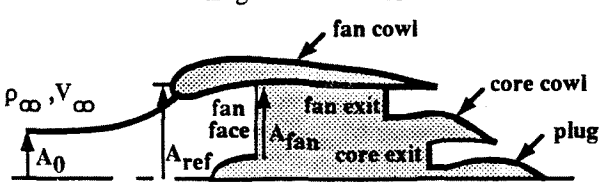

- Figure 2 -

The fan face is a subsonic outflow surface for the computation domain. Four characteristic relations are used and the system is closed by setting the fan mass flow.

The fan and core exits are subsonic inflow surfaces for the computation domain. One characteristic equation is kept and the closure of the system is achieved with the stagnation conditions : fan and core pressure ratios, fan and core total temperature ratios versus upstream total temperature and directions of the velocity vectors on this particular faces.

This code has been validated on various configurations through experimentation / computation comparisons [1] [2] [7]. Two examples are developed hereafter. This tool is used in an industrial manner and is heavily included in the development process of a project.

4.Application to a VHBR engine integration

4.1 Introduction

The new propulsion system concepts that are very high bypass ratio (≈10) engines (VHBR) to ultra high bypass ratio (≈20) engines (UHBR) offer today good economical advantages (specific fuel consumption savings, propulsive efficiency,...) while providing better environmental compatibility (emission, noise,...).

However their integration on aircraft leads to stronger engine/airframe interference caused mainly by a closer position of the nacelle relative to the wing. It is necessary to preserve a sufficient ground clearance for underwing-mounted engines with such increased fan diameter. Moreover, the nozzles (fan and primary) are working with lower pressure ratio than conventional engine but, even if jets are less energetic, their size and proximity create higher wing interaction.

It should be damaging that economical benefits obtained with the engine are canceled by severe aerodynamic interactions.

Two years ago, theoretical and experimental approaches have been prospected by Aerospatiale for the study of the integration of a 115" VHBR engine on an Airbus twin.

Engine positioning under the wing has to fulfill several mechanical constraints (ground clearance, turbine burst, weight, loads on mounts and systems crossing)(fig 3). A large part of aerodynamic integration difficulties comes from above limitations.

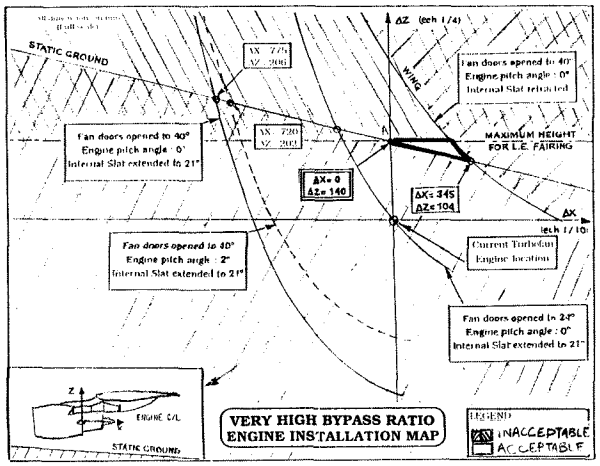

- Figure 3 -

4.2 W/T Tests

Within a cooperation with GE, Aerospatiale has conducted installation tests in the S1 MODANE (France) transonic wind tunnel on a half-model at 1/17.5 scale, fitted with powered (ø180mm Turbine Powered Simulator (TPS)) and through-flow nacelles, representative of this VHBR engine, and with a powered (ø142mm TPS) nacelle, representative of a current turbofan, used for reference. The tests objectives were to assess wing/nacelle relative location influence (only axial effect) and the jet effects for the VHBR engine and then the VHBR/conventional turbofan engine installation drag comparison.

The model was fully instrumented with static taps on wing, close to the engine position, and nacelle cowlings. All test results are given for cruise conditions.

Figure 4 shows the basic location of the VHBR engine under the wing , relative to the current turbofan position : fan exit stations are coinciding.

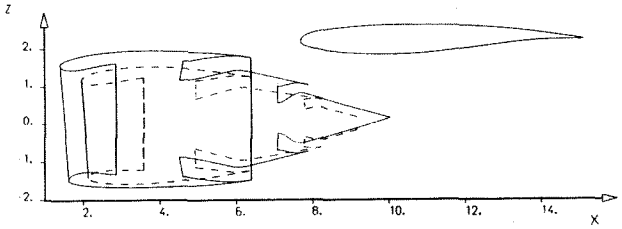

- Figure 4 -

The alternative aft position (1/2 m full scale) tested (in TPS configuration) has proven that the axial location effect was very small on the installation drag, about 0,2% of total A/C drag. On the wing lower side, moving aft the nacelle leads to an acceleration of the flow up to around 20% of chord, corresponding to the core exit station location, followed by a slight deceleration to recover the basic location pressure level at the trailing edge (fig 5). The detected acceleration is due to the jet velocity and displacement which increases the natural channel effect between fuselage and powerplant. On the upper surface, inboard side, the shock occurring at 35% chord is a little stronger than for the basic location.

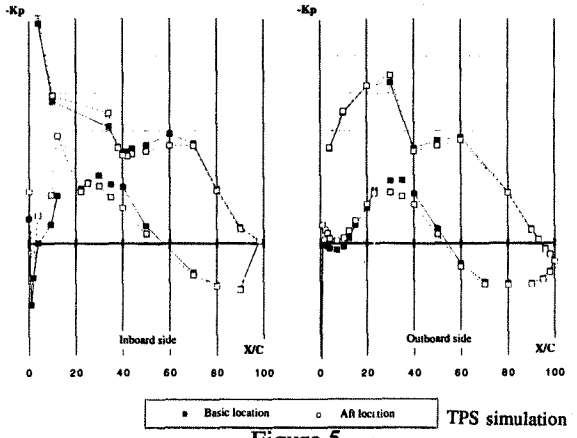

- Figure 5 -

In order to estimate the pylon leading edge fairing contribution, an alternative pylon with different crest line, but not taking into account the aircraft constraints, has been tested (only in TFN configuration): this modification has allowed to reduce significantly the installation drag although no effect on the lift has been detected. The only noticeable effect on the wing is situated on the upper surface, inboard side (fig 6) : the first shock occurring before 10% of chord with baseline pylon has disappeared with modified pylon.

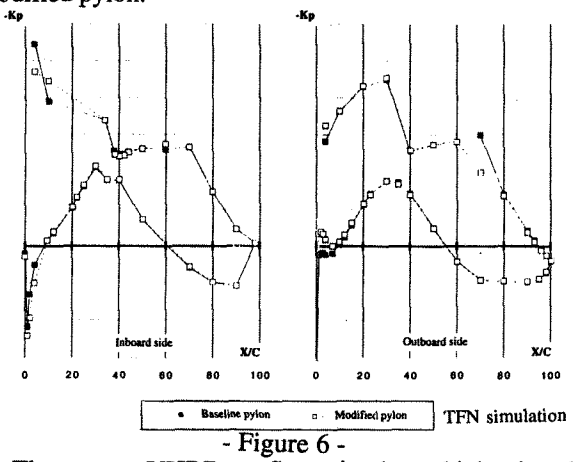

- Figure 6 -

The present VHBR configuration has a higher installed drag than the current turbofan (0.8% of aircraft total drag in average) and an additional lift loss of about 0.05 degrees in cruise conditions (fig 7a, 7b).

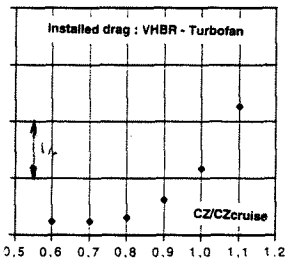

- Figure 7a -

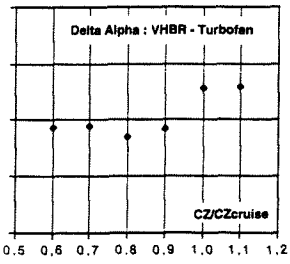

- Figure 7b -

The comparison of clean wing, current turbofan and VHBR under-wing engines in terms of wing pressure distributions is shown in figure 8. All effects of conventional engine installation are enhanced by the closer location and larger dimension of VHBR engine. On the upper surface, the shock moves forward, pressure recovered after that is higher. Clean wing level are reached at about 75% of chord, as current turbofan. On the lower surface, inboard side, jet energy seems to be more influential than plume proximity, since the VHBR engine configuration leads to a lower flow acceleration after the leading edge. Nevertheless the following compression is more severe.

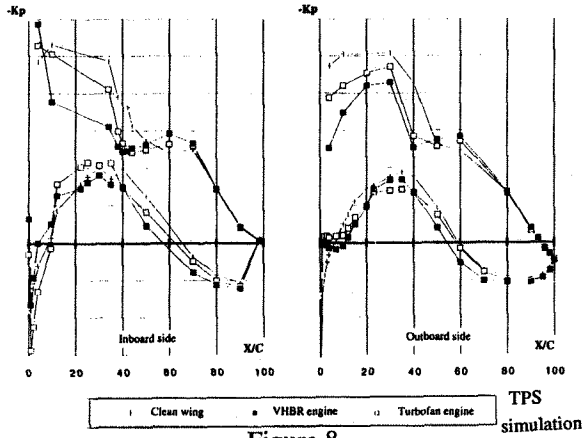

- Figure 8 -

4.3 CFD simulations

Previous communications [1] [2] have already presented these W/T / CFD results comparison, and then only a sum-up of them will be given here.

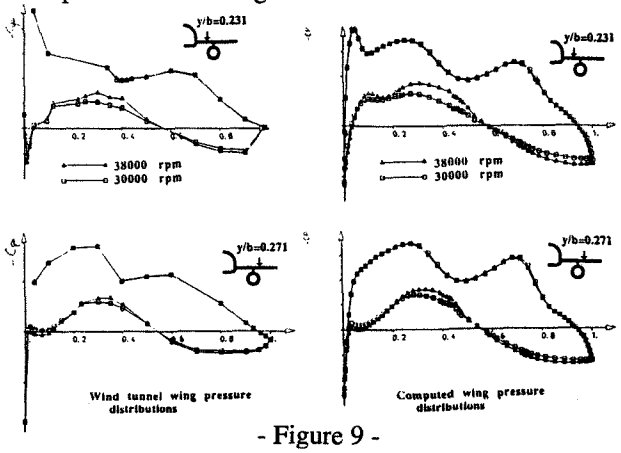

- Figure 9 -

Most of tests data have then been compared with CFD results on a 1400000 points grid representative of the previous VHBR configuration, including fuselage, wing, pylon, and full geometry of the nacelle. The Euler model used allows a very good simulation of the engine jets (geometry and stagnation conditions) so that high wing/plume interaction can be assessed by computation.

For instance the influence of an engine speed variation can be pretty well predicted with SESAME as can be seen on figure 9, which compares wind tunnel and CFD pressure distributions on two wing sections located on either side of the engine.

4.4 Conclusion

This study has estimated with both experimental and numerical tools the effect of the integration of a Very High Bypass Ratio 115" engine on a transonic commercial aircraft. Installation drag of this first iteration configuration (no optimization has been performed) was only about 0.8% of total aircraft drag more than a current turbofan engine, but further advanced design (pylon) supported by future W/T tests and CFD analysis could cancel this extra-drag.

5. Application to the thrust vector deviation impact on engine airframe integration

Up to now, civil airframers have requested to engine manufacturers that their engines deliver a thrust on the engine axis, i.e. having a 0° thrust vector angle. The engine is then settled under the aircraft in a way that thrust is close to wind axis at cruise so that a maximum part of the thrust achieved by the engine is used to fight the drag.

During the early wind tunnel tests of the studied aircraft, nozzles calibrations have shown some deviation of the TPS model thrust. A large part of the installation effect measured with the corresponding wind tunnel test could have been explained with this misalignment of the vector. This result was the starting point of the thrust vector angle (TVAN) study which aim was to clear the following questions : Is the 0° TVAN the optimum and, if not, what is the good angle?

Supported by AIRBUS industry, this study was led in cooperation with CFMI. Its subject deals with the jet efflux interaction with the aircraft. TPS technic was a necessity for the wind tunnel test and EULER solver code was requested for the CFD engine simulation.

As a definition, the thrust vector angle is assumed to be positive if the force is in lift direction.

5.1 Test hardware definition

The test program included four different TVAN nozzles: -6°, -4°, 0° and +4° (fig 10).

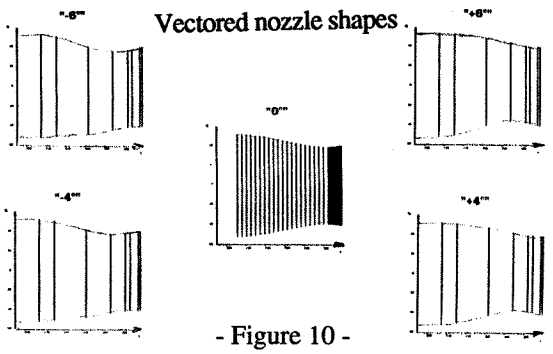

- Figure 10 -

The deviation of the jet was obtained by modification of the inner shape of the exhaust nozzle. Last part of the fan cowl was affected and its definition was no more axisymmetric. Design rule, resulting from an intensive CFD work realized at the cruise point, was based on the choice of a non straight section center line. Its final slope is directly linked to the TVAN and the smoothness of the center line contributes to the quality of the nozzle flow.

The TPS internal mixing design has no particular impact on nacelle calibrations. We still use the same couples of laws but some thermodynamic parameter calculations requires specific instrumentation. The internal mixing station is equipped with static pressure taps on the outer and inner lines of the fan duct. Four of them are on the fan cowl and four others on the core cowl. The operant tap measurements are introduced into the calculation loop leading to the determination of the exit mass flow coefficient, the mixing temperature and so the corrected total mass flow, the total ideal thrust and the exit thrust coefficient.

5.2 Test specific technic

During the calibration test, specific laws could be established with the mixing station parameters. But the reliability of wall static taps in TPS is difficult to achieve due to bearings oil natural leakages and thin ice accretion on core cowl. A wind tunnel data reduction based on both laws have shown no significant difference. For these two reasons, we have decided to keep the original couple of calibration laws taking into account the fan and core mass flows, the TPS nacelle thrust and the fan nozzle pressure ratio. Mixing parameters are calculated for survey purpose.

All calibration forces plotted together give an overall angle of thrust deviation. This angle is determined with a ±0.25° precision and is assumed to be constant for the cruise range of nozzle pressure ratios. This angle is directly used in the wind tunnel data reduction, i.e. balance measurements are corrected from ram drag and nacelles net thrust on both engine axis and vertical axis. This last correction is calculated from engine axis net thrust and the average thrust vector angle.

For the quality of the results, the reference is tested between each TPS model configuration. Jet effect calculation is realized as usual : difference between the aerodynamic coefficients measured with the TPS configuration and the reference one.

5.3 EULER solver validation by laser tests

CFD work has been conducted with an EULER code on model and aircraft configurations. Full validation of the code was necessary and it could be obtained by local velocities direction and magnitude comparison between test and computation results. A laser test conducted by Aerospatiale in the S4b Modane static bench facility made it possible to collect a good data-package in order to ensure a reliable CFD code validation.

The TPS operating conditions during the laser tests have been introduced as input of CFD calculations, whose objectives were to determine the following input effects : total pressure and temperature distortion, velocity direction including swirl (only on core). All results are given for a cruise fan nozzle pressure ratio of 2.3.

Computed and measured axial and vertical velocities have been compared at two stations : exit nozzle station and downstream station (≈one exit nozzle diameter behind exit plane), some results of exit station are discussed below.

On figure 11, lines represent iso axial component of velocity (u). Pressure and temperature distortions have the most significant effect on axial velocity, the best comparison being obtained with the full distortion (radial and circumferential) measured during tests. The rotation of flow induced by the swirl leads to a little deceleration locally around the plug.

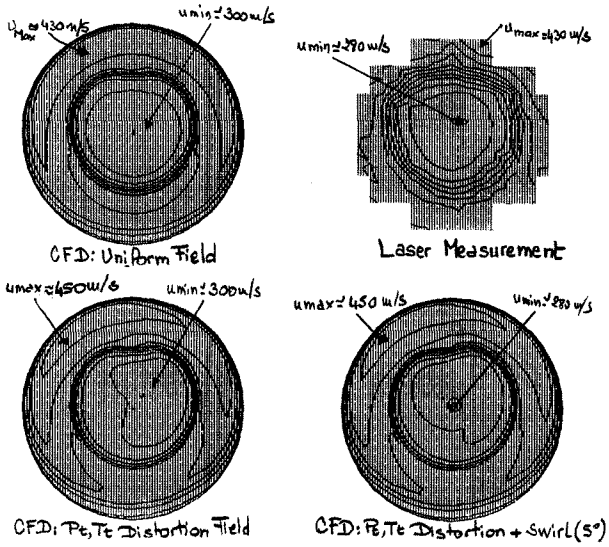

AXIAL VELOCITY : LASER AND EULER RESULTS COMPARISON

- Figure 11 -

On figure 12, lines materialize the iso vertical deflection angle values (arctg(w/u)). It is clear that the swirl is absolutely necessary to precisely simulate the vertical velocity. The entrainment effect of the flow by the rotating turbine is correctly reproduced by Euler solution, even if it is less diluted because of the lack of viscosity.

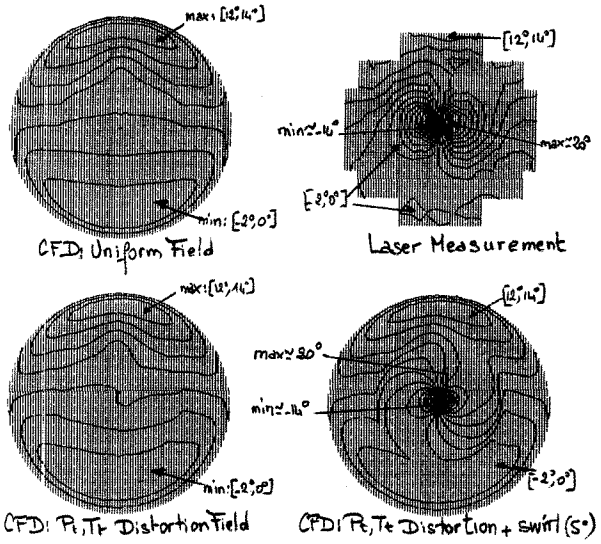

LOCAL VERTICAL DEVIATION : LASER AND EULER RESULTS COMPARISON

- Figure 12 -

Pressure and temperature distortions effects on thrust vector direction have been also investigated after previous calibrations tests with four vectored nozzles (-6°, -4°, 0° and 4°). Associated Euler computations have shown the little impact of total temperature (which is above all a significant parameter for viscous effect) and the preponderant effect of circumferential pressure distribution on the thrust vector angle [2] [7]. This result is illustrated on figure 13 where circumferential pressure distortion at fan exit station permits to reach the maximum effect on TVAN, about +0.5°.

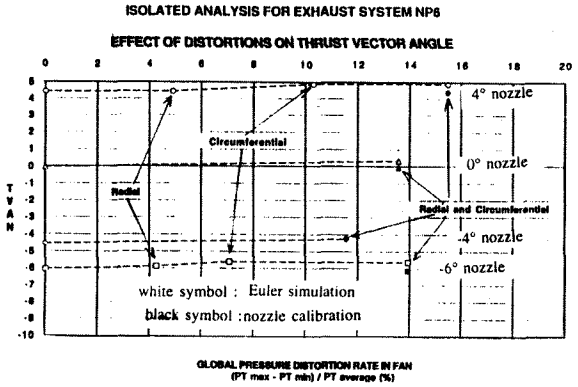

- Figure 13-

However, although a good modelling of distortions is necessary to simulate local flow description (axial velocity, local vertical deviation), CFD analysis and isolated W/T calibration data comparison show that the uniform field calculation gives generally a very close estimate of the thrust vector angle, as indicated in table 1. This is due to a balance between unsimulated effects as viscous effects (inside walls, mixing layers,...), all values, measured and calculated, being still within the bench accuracy.

Simulation conditions	+4° nozzle	-6° nozzle
Wind tunnel	+4.400°	-6.150°
CFD : uniform field	+4.438°	-6.061°
CFD : Θ distortion	+4.884°	-5.630°
CFD : r distortion	+4.446°	-5.903°
CFD : Θ+r distortion	+4.896°	-5.637°

- Table 1-

The close agreements between Euler calculations results and laser measurement data lead to the complete validation of the code, intensively used for the thrust vector CFD study described now.

5.4 Isolated tests and CFD : analysis

Euler calculations are performed on isolated nacelle configuration, first, to simulate powered nacelle calibration tests. However, their relative low computation cost, their easy set-up and post-processing (induced by reasonable mesh size, about 180000 points) compared with complex installed configuration permit to investigate various phenomena, as the distortion effect on thrust vector direction mentioned above.

Another interesting study is the evolution of the TVAN versus the nozzle pressure ratio, whose CFD results have been compared with recent available exhaust nozzle static tests data. Two nozzles, a baseline (0°) and a vectored one (≈-4°), and three pressure ratios (1.5, 1.6 and 2.4) have been computed (with uniform pressure and temperature field at M∞=0.15). Corresponding tested pressure ratios were ranging from 1.2 to 2.6. Figure 14 shows a very good agreement between experiment and Euler results.

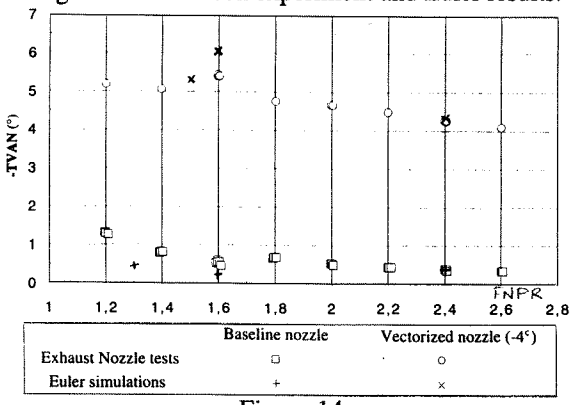

- Figure 14 -

For both nozzles, the discontinuity at FNPR≈1.6 appearing during tests is well represented with Euler code, even if effects are amplified without viscosity simulation. The local mach number distribution in the plane of symmetry of the -4° nozzle is given figure 15a for FNPR=1.6 and figure 15b for FNPR=2.4. The first case (FNPR=1.6) corresponds to the beginning of the choke and a sonic line is emerging close to the upper part of the throat nozzle, where the jet is deviated, the flow remains subsonic downstream. At FNPR=2.4 the nozzle is fully choked, the sonic line stretches all across the throat nozzle and the jet is supersonic downstream. Compared to the last case, the choking nozzle presents a dissymmetric distribution of pressure and velocity in the jet that leads to a higher magnitude of thrust vector angle than in more established nozzle conditions (non choked or fully choked). The equivalent analysis on the baseline nozzle has shown that it was choking first in its lower part. That explains the up step for -4° nozzle and down step for 0° nozzle at FNPR=1.6.

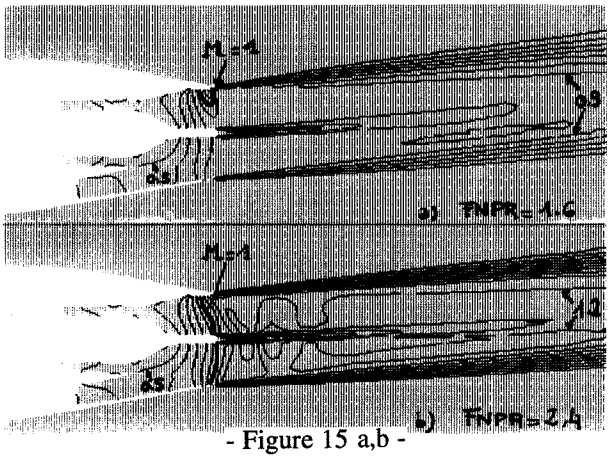

- Figure 15 a,b -

Thus, Euler numerical simulation has made possible to understand unexpected and surprising tests results, with a very good representation of jet flows. To achieve a still better estimation of phenomena including viscosity effects, the use of a Navier-Stokes code would be necessary. If it is conceivable on isolated configurations, industrial use of such a solver with sufficient quality on complex installed configurations is not ready.

5.5 Installed test data analysis

Two wind tunnel test campaigns have been performed. Results of each tests are in agreement and indicate the same trends.

5.5.1 Forces

Going from +4° to -6° nozzle on outboard position shows a jet effect decrease at cruise point of nearly 2% of aircraft drag (fig 16). In particular, a change of TVAN of the current 0° nozzle to a -4° one reduces the aircraft drag by 1%. The minimum is reached when the jet is directed toward the wing which is against any logical feeling.

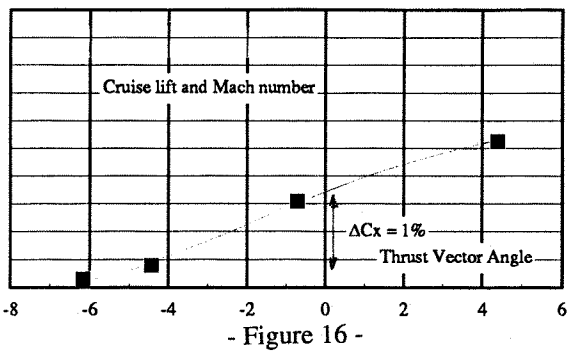

- Figure 16 -

At the cruise angle of attack, the lift coefficient is slightly affected (fig 17) with a minimum for the 0° nozzle. Going from a 0° nozzle to a -4° increases the lift by 0.3% of aircraft cruise lift.

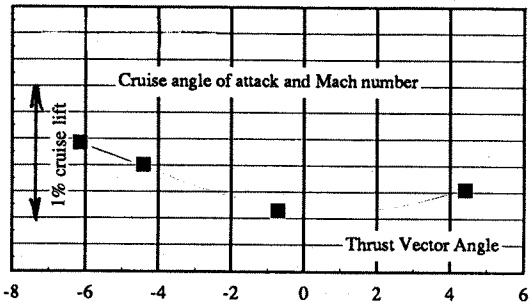

- Figure 17 -

The same analysis have been performed on a dual engine simulation test including current aircraft definition (both nozzles having no thrust deviation) and the foreseen improved version (both nozzles having -4° TVAN)(fig 18).

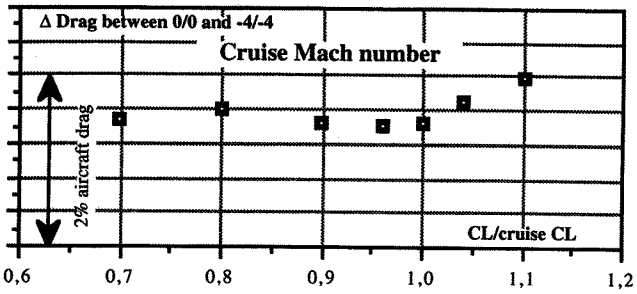

- Figure 18 -

Jet effect drag is not drastically modified and the reduction is about 1.4% of aircraft one. This illustrates the great sensitivity of the outboard engine versus the inboard one which could be attributed to the difference existing in the chord versus engine size ratio for both pods.

Lift modifications remain light (fig 19). In particular, at cruise, a nozzle change on the aircraft from 0° to -4° TVAN would increase lift by a bit less than 0.4% of aircraft cruise lift.

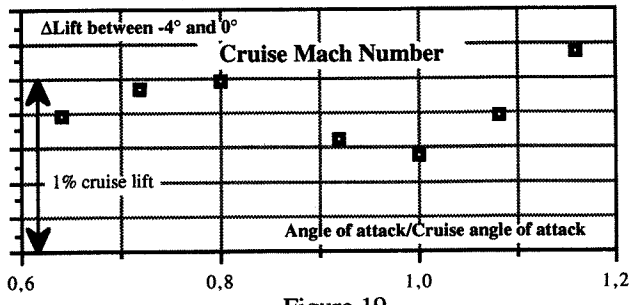

- Figure 19 -

Great care, as for all tests, have been taken for its completion. Each data point has been at least done twice. Calibrations laws are also the result of two independent sets of points. On another hand, due to the high nozzle pressure ratios used during the high speed test, the exhausts are choked and no outside perturbation could interfere with TPS working. This has been verified through installed computations. Wing pressure taps analysis has been performed having in mind the search of an answer to this drag improvement.

5.5.2 Wing static pressure distribution

The wing model is equipped with one raw of static pressure taps on each side of the engines.

When looking at inboard engine, one could note that at the cruise point, between 20% and 50% of local wing chord on the inner surface, velocities are a bit lower for -4° nozzle than 0° and TFN ones (fig 20). In addition, on inboard side, -4° and 0° nozzles seem to have lower velocity than TFN at the suction peak. Wing upper surface pressure distribution is not affected by TVAN nozzles at cruise point. But, we shall insist on the fact that pressure effects on wing due to thrust vectoring are limited close to inboard pylon.

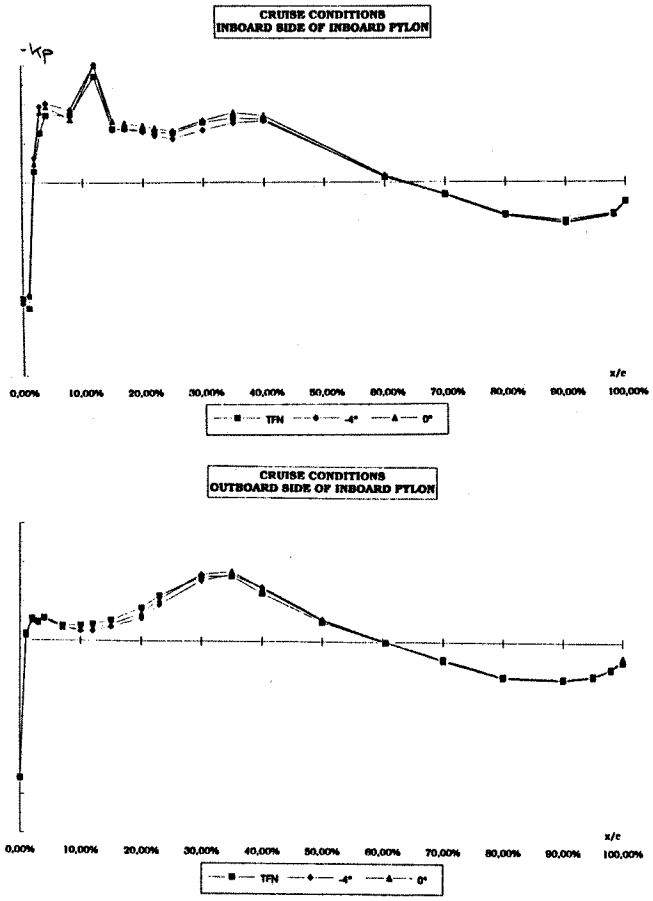

- figure 20 a,b -

Four different nozzles have been tested on outboard position (fig 21). On inboard side and lower surface of outboard pylon the maximum effect appears at the suction peak. At cruise CL, nozzles are in the following order : +4° at the highest level, -4°, 0° and -6° for the lowest level. Compression behaviour after the peak are different : +4° and -4° have a common sharp aspect while 0° and -6° have lazier shapes.

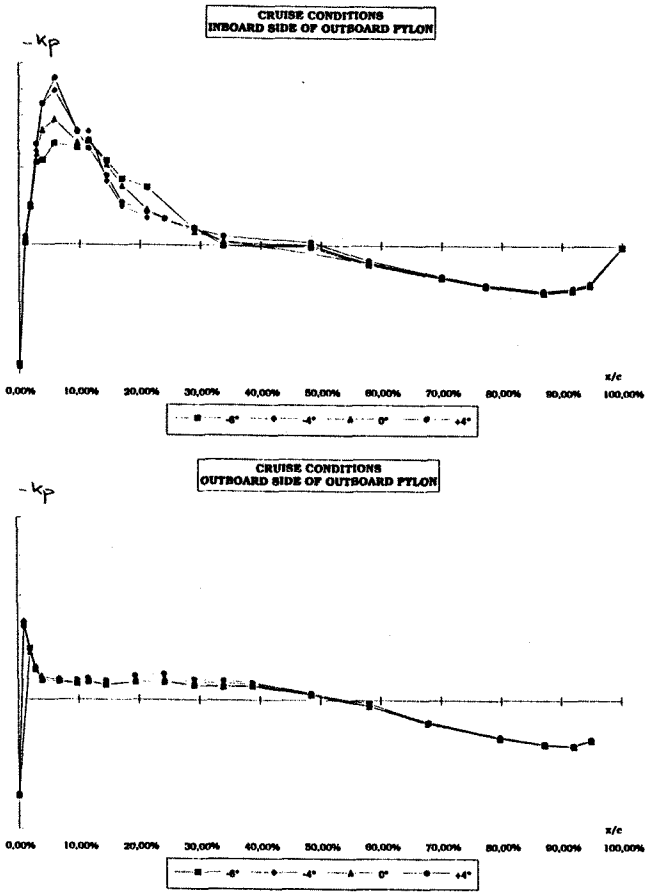

- Figure 21 a,b -

On outboard side of outboard pylon, the suction peak is lower and nozzle order is reference at the top, then -4°/-6° rather equivalent, +4° and 0° at the bottom. After the suction peak, between 10% and 40% of chord, some differences in pressure level could be observed : +4° at the top, reference / 0°, then -4° and -6° nozzles. Nozzle classifications do not match with the drag improvement, the lift modification or the TVAN deviation.

However, static pressure distribution on the wing is unable to explain drag benefit due to vectored nozzle. Effects are observed, especially on outboard position. In addition, flow behaviour around the nacelle is highly dependant upon the jet direction but no investigation has been realized during these wind tunnel tests. In fact, negative TVAN seems to have a correcting action on difficult flow areas. It creates a kind of flow blockage for important velocities flow on inner side of the inboard pylon/wing junction. At the opposite, on the inner side of the outboard pylon, it sucks the flow and increases its velocity while stabilizing it. Pressure analysis is difficult due to the balance between these two opposite effects : blockage and sucking. Depending on the relative position of the engine versus the wing, and the incoming flow conditions one of these two effects prevails.

Wind tunnel measurements are as detailed as possible. Observed phenomenon are very small and under usual experimental technic possibilities. A large part of complementary information could be obtained through CFD analysis. This was the object of a parallel approach.

5.6 CFD work

Euler analysis have been also performed with different vectored nozzles installed on aircraft to assess the influence of jet deviation.

At cruise conditions [2], computations lead to a correct prediction of the lift increase trend when passing from a +4° to a -6° nozzle. Wing pressure distributions on either side of the outboard engine were correctly calculated except at the suction peak probably due to a viscous phenomenon which cannot be reproduced by an Euler simulation. Other CFD technics, including boundary layer simulation, would certainly be preferable. Such computations are not on industrial use for installed configurations for the moment.

More recently, low speed analysis have been performed in order to check jet position with respect to extended flaps.

The geometry used for these calculations includes the fuselage, inner and outer engines and a cambered wing which is representative (same lift distribution) of the wing with extended slats (23°) and flaps (32°). The cambered wing was designed by deforming the clean wing so that its contour follows slats and flaps contours at a given angle position (23° for the slats and 12° for the flaps) as can be seen on figure 22. The flaps 12° extension allows to get the correct lift coefficient for the cambered wing.

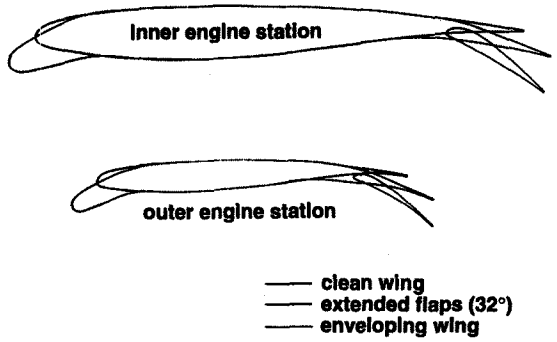

- Figure 22 -

Two nozzles have been installed both on inner and outer engines. These are the 0° and -4° nozzles previously described.

The corresponding grids are made up of 69 domains and 540000 points which is quite coarse for such a complex configuration. Mesh refinements have been concentrated around the two engines (fig 23).

SESAME analysis were run on a CRAY C90. The convergence was reached for both after 1200 iterations which corresponds to 2h30 cpu time. Take-off flow conditions were used.

Figures 24 and 25 compare plume positions for 0° and -4° nozzles at the inner and outer engine span stations.

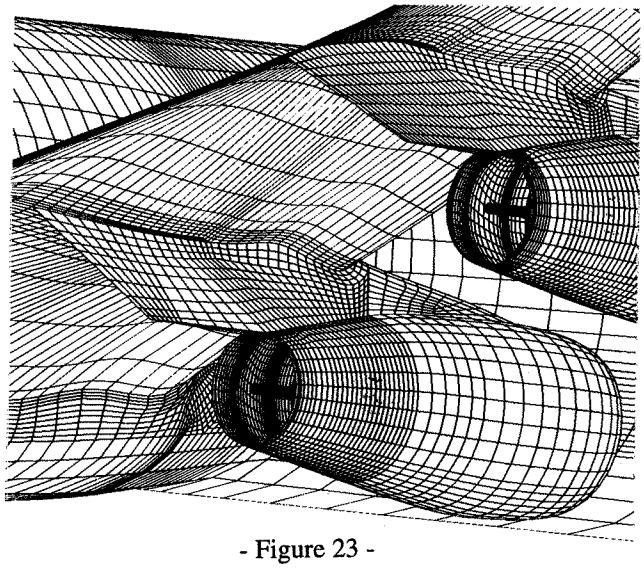

- Figure 23 -

Actual positions of 32° extended flaps are also plotted. One observes the same phenomena as for isolated nozzle calculations. Nozzles are not choked because of low values of total pressure ratios. One consequence is that airframe influences nozzle flow as can be seen by comparing fig 24a and 25a or fig 24b and 25b : Mach contours are slightly different in the inner and outer nozzles. Thrust vector angles (TVAN) are different as well : 0° (resp. 4°) nozzle actual TVAN is -0.29° (resp. -5.02°) in inner position and -0.53° (resp. -5.25°) in outer position.

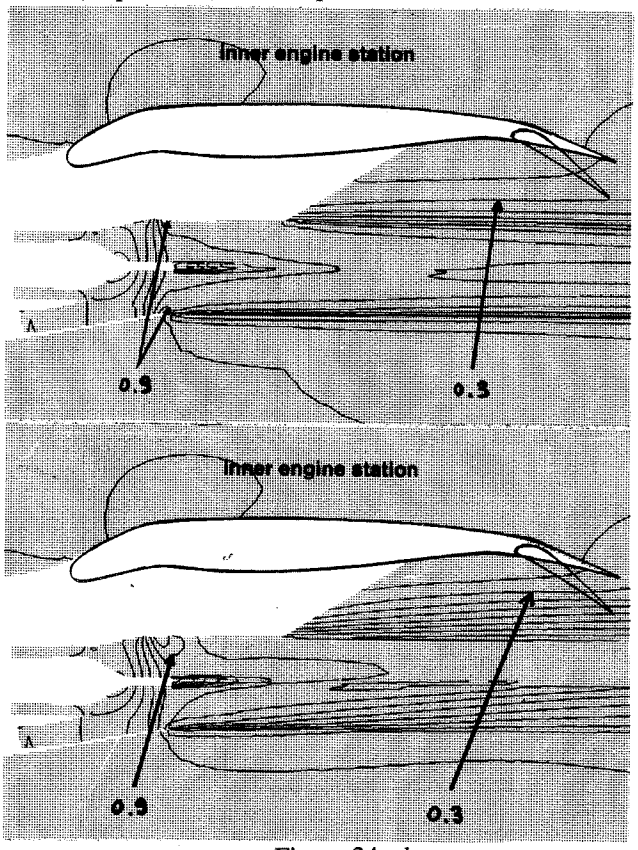

- Figure 24 a,b -

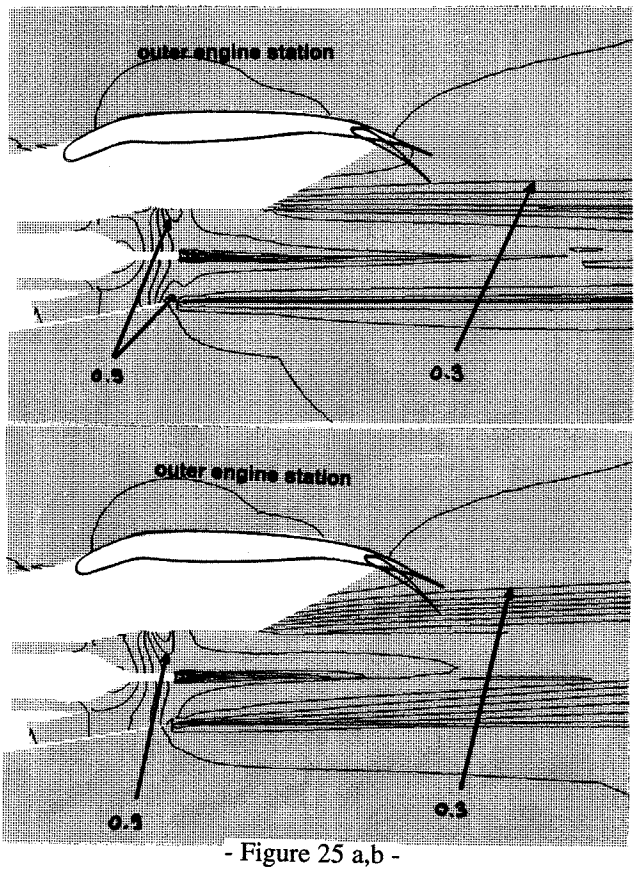

- Figure 25 a,b -

Impact of plumes on the flaps seems to be not critical for both nozzles. Jets coming from 0° nozzles remain always below the flaps. For -4° nozzles, the worst situation occurs near to the inner engine because the flap is situated in a rearer position behind the nozzle exit plane than for the outer one. But even in this case flap lower point remains in the mixing layer between the jet and outer flow.

6. Conclusion

Yesterday, CFD and experimentation were two different worlds.

Today, test technics have to be more and more precise in the search of aerodynamic improvements. In the engine integration domain, the complex TPS technic has become a basic test tool.

By the same moment, due to computers power increase, CFD possibilities have progressed, and engine jet simulation on installed configuration are now common EULER computations.

These facts have changed our working process. CFD reduces the experimentation work by selecting potentially interesting engine / airframe integration configurations among a large panel of them. It helps model design by verifying TPS nacelle flow quality and compatibility with the foreseen study. Then, CFD brings flow behaviour informations in unexplored or unexplorable areas.

But, experimentation will always remain essential for numerous reasons : drag and more generally aerodynamic

coefficients levels, flow separations, highly viscous or unsteady flows.

Today, wind tunnel activity could not be replaced and the yesterday enemies have reasonably learned to work together.

Acknowledgments

A large part of the work leading to the preparation of this paper was supported by AIRBUS INDUSTRY, GENERAL ELECTRIC, SNECMA and CFMI.

References

[1] X. Monthus, P. Colin, P. Mogilka, A. Molbay-Arsan: "Utilisation des méthodes de calcul pour optimiser l'installation motrice des avions de transport", AGARD Symposium on Recent Advances in Long Endurance Operation of Aircraft, The Hague, May 24-27, 1993.

[2] P. Colin, P. Mogilka, A. Molbay-Arsan : "CFD analysis of engine / airframe interference for advanced integration studies on transport aircraft", Royal Aeronautical Society Conference, Bristol, September 1-3, 1993.

[3] D. Bertin, J. Lordon, V. Moreux : "A new automatic grid generation environment for CFD applications", AIAA-92-2720-CP, 10th AIAA Applied Aerodynamics Conference, 1992

[4] D. Bertin, C. Casties, J. Lordon : "A new automatic grid generation environment for CFD applications" Numerical grid generation in computational fluid dynamics and related fields, Ed N.P. Weatherhill, P.R. Eiseman, J. Häuser, J.F. Thompson, pp 391-399 Pineridge, 1994.

[5] V. Couaillier : "Multigrid method for solving Euler and Navier Stokes equations in two and three dimensions", 8th GAMM conference on numerical methods in fluid dynamics, Delft September 27-29, 1989

[6] A.M. Vuillot, V. Couaillier, N. Liamis : "3D turbomachinery Euler and Navier Stokes calculations with a multi-domain cell centered approach", 29th AIAA/SAE/ASME/ASEE joint propulsion conference, AIAA 93-2576.

[7] A. Molbay-Arsan : "Simulation numérique d'effets de jets réacteurs par résolution des équations d'Euler autour de configurations motorisées d'avions de transport en régime transsonique" thesis submitted on November 93.